Using Hotmelt-Inkjet as a structuring method for higher efficiency industrial silicon solar cells

J. Specht, D. Biro, N. Mingirulli, M. Aleman, U. Belledin, R. Efinger, D. Erath, L. Gautero, A. Lemke, D. Stüwe, J. Rentsch, R. Preu;
Fraunhofer Institute for Solar Energy Systems; Freiburg, Germany

Abstract

A procedure was developed to form openings in dielectric layers for subsequent contact formation based on inkjetting hydrocarbon wax. Basic investigations on the process focussing on obtaining the minimal feature size are presented.

Continuous fine line openings below 20 µm width in the mask were obtained, which allowed for wet chemical etching of the underlying anti-reflective coatings. Subsequently nickel and Silver plating were used to form ohmic contacts, leading to a width of the metallization of down to about 30 µm. The results were achieved on micro-structured silicon surfaces covered by a silicon nitride layer commonly used in the photovoltaic industry.

Introduction

Dielectric layers for high effiency lab-scale silicon solar cells are commonly structured by photolithographic means. For industrial application of high efficiency cell concepts, low-cost and high throughput technologies are required. Inkjet structuring combines high throughput like e.g. screen-printing and high precision and is thus a candidate for structuring technology for the next generation industrial solar cells.

A key feature of next generation industrial solar cells is a new front contact layout. In order to reduce both shadowing losses and contact resistance between metal and silicon and to account for line conductivity, a two layer concept has been presented by Glunz et al. [1]. A thin low contact resistance seed layer is deposited and subsequently plated to account for line conductivity. With state-of-the-art screen-printing a front contact grid line width of 80 µm can be achieved. Inkjet technology has the potential to reduce line width and hence obscuration losses.

In order to reduce silicon consumption next generation industrial silicon solar cells will be thinner, consequently mechanical impact must be minimized. Since Inkjetting is a contact-less printing technology, it has a clear advantage over screen printing.

Figure 1 shows two process sequences to create two layer front contacts with inkjet technology. The substrate consists of a p-doped Si-wafer with a highly doped n-type emitter layer covered by a silicon nitride-layer (SiN) of about 70 nm thickness as anti-reflective coating. The inkjet-mask, consisting of hydrocarbon wax that is resistant to hydrofluoridic acid (HF) is jetted onto the SiN-layer. The mask features line openings at the desired position of the contact grid. The SiN is then etched with hydrofluoric acid.For the seed layer formation by means of inkjetting there are two options: 1. A stack layer of TiPdAg is deposited on the substrate with inkjet-mask as presented by Biro et al. [2]. In a subsequent Lift-Off process the ink-mask is removed with the metal on top of it. 2. The inkjet mask is removed with a solvent. Nickel is deposited by electroless plating, which is a self-aligning process,

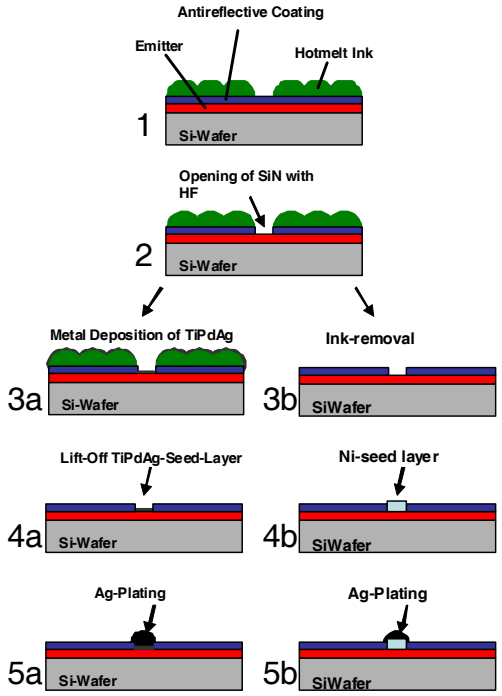

***Figure 1**: Two concepts for front side metallization basec on Inkjetting hydrocarbon wax: a) Metal deposition of TiPdAg, b) Electroless nickel-plating*

i.e. it is deposited where the SiN-layer is fully opened. Either way the seed contacts are used to grow a bulk silver finger on top to ensure high line conductivity.

In the following we show our investigations of droplet and film characteristics dependent on printing parameters as well as etching of dielectrics to create line openings for front contacts. Finally the results of seed layer deposition according to Process b are presented.

Droplet and film characteristics

A labtype Schmid DoD300 inkjet system was used for the following investigations. It features a piezo drop-on-demand printhead. Tiff-files were used as input files. The hotmelt ink used consists mainly of hydrocarbon wax and is jettable at temperatures between 70…95°C. The substrate is placed on an xy-table, which has a fast and a slow axis. The fast axis is referred to as the printing direction. The native resolution of the printhead is 50 dpi. The table can be moved perpendicular to the printing direction with a min. step width of 5 µm. For example, a closed film of hydrocarbon wax is printed in the following manner: each nozzle

prints one line. The table is then moved perpendicular to the printing direction and another line is printed. This process is repeated until the area in-between two nozzles is covered. In order to print areas exceeding the printing head width the table is then moved by the distance between the outer nozzles. The resolution in printing direction and perpendicular to it may be set individually.

In the following the influence of piezo pulse shape on droplets will be discussed. The operation of the piezo element compressing the pumping chamber is defined by a voltage pulse of trapezoidal waveform, and is defined by the following parameters: the rise time t_{rise} is characterized as the time between the onset until 90 % of the set piezovoltage is reached. The fire pulse width t_{FPW} is the time from the voltage onset to the point where the voltage drops below 90 % of the set piezovoltage. This means, that t_{rise} is part of t_{FPW}. A higher voltage increases the droplet speed and volume [3]. As a trend in our assembly, an increase of t_{FPW} leads to larger droplets, as can be seen from Figure 2. For fire pulse widths between 7.5 and 10.5 µs the drop volume is almost constant at a piezovoltage of 95 V. The fall time t_{fall} is marked by a decreasing piezovoltage from 90 % to 10 %.

Figure 3 shows a droplet on a polished silicon surface. It can be observed that the droplet has a spherical segment shape with a larger radius than the liquid drop, which can be observed in a stroboscopic camera. According to Gao and Sonin, the ink is still liquid when hitting the surface [4]. The droplet spreads and solidifies on the surface. When reheating droplets above the melting point the drops were observed to spread even further. As a conclusion the droplets solidify before they reach equilibrium in the liquid phase. Therefore solidification must be more dominant for the resulting shape of the solidified droplet than wetting of the substrate surface. Drops have a volume ranging from 16 to 30 pL, depending on the settings. The radius of the solidified droplet on the substrate ranges from 24 to 32 µm.

When positioning drops with overlap, continuous lines can be formed as pictured in Fig. 4. In printing direction the droplets do form a continuous surface. The situation is different when lines are printed perpendicular to the printing direction. The structure of the single droplet is more prominent compared to lines printed in printing direction. It may be described as stacked coins, slightly melting into each other. Hence, the droplet must be at least partially liquid when hitting the surface and the previously deposited and solidified drop. The time between deposition of neighbouring droplets perpendicular to the printing direction exceeds the time in printing direction by several orders of magnitude, depending on the image dimensions.

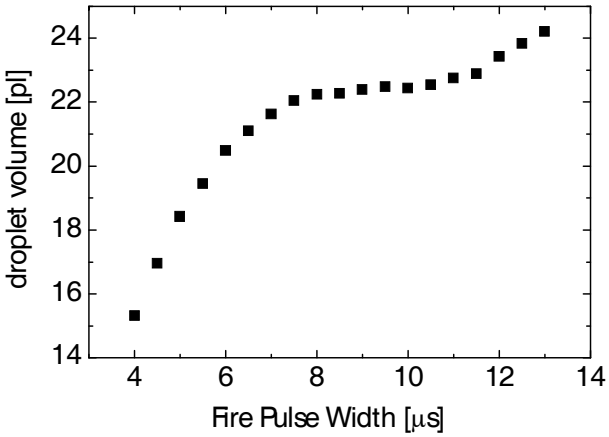

Figure 2: *Influence of fire pulse width on droplet volume. The droplet volume increases with fire pulse width. The increase is small between fire pulse widths from 7.5 to 10.5 µs*

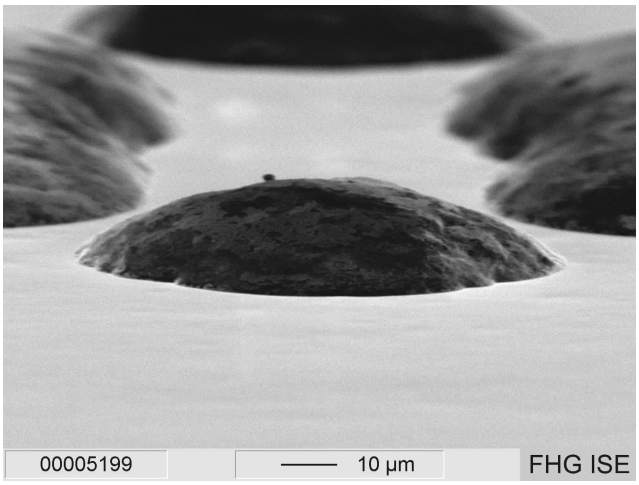

Figure 3: *SEM picture of a hotmelt droplet on monocrystalline silicon surface. The droplet forms a contact angle below 90°. The surface of the droplet is uneven.*

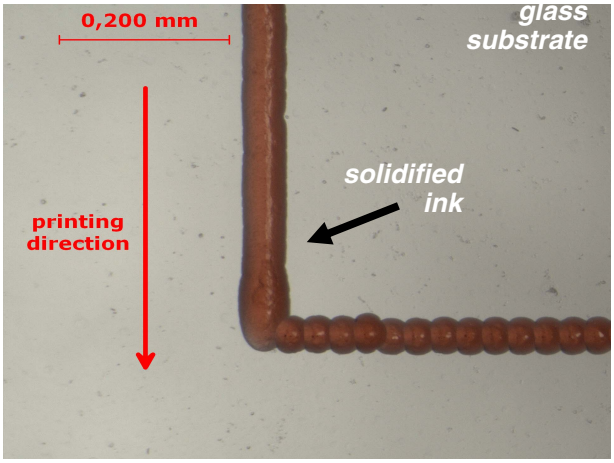

Figure 4: *Printed lines in and perpendicular to the printing direction. In printing direction droplets coalesce, whereas perpendicular to it they maintain drop shape.*

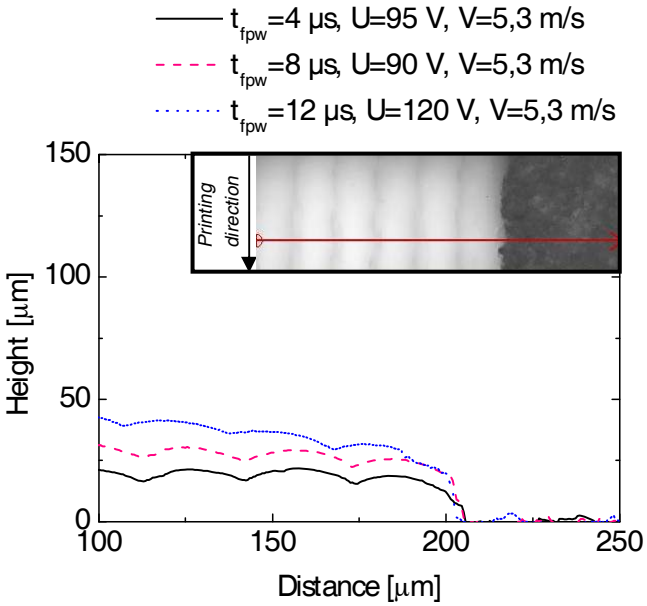

Figure 5: *Film thickness dependent on droplet size. The profiles were measured perpendicular to the printing direction. The film thickness increases with droplet volume and ranges between 20 and 40 µm.*

For many applications it is important to form closed films to cover larger areas which are entirely dense against HF. Even tiny uncovered areas may damage the solar cell by harming a functional layer in a subsequent etching step. Figure 5 shows confocal measurements of the film topography for different parameter sets. All samples were printed with a droplet speed of about 5.3 m/s at 85°C. The parameters were chosen to have three different droplet sizes at the same droplet speed, resulting in full coverage films. The small image shows the position where the profile was measured. The film thickness increases with droplet volume and ranges between 20 and 40 µm. The HF-density of the films described was found to be independent of the printing parameters. As a result the smallest droplets can be used to achieve smoother edge definition and small feature sizes, with the restriction that HF-density is also given in lateral direction. Geometrical considerations lead to a droplet pitch of less than 0.7 times the diameter d to achieve 100% coverage. We have tested films of different pitches on substrates with dielectrics etching 3 min in 20% HF. The dielectrics remained unaffected when a smaller pitch of ~0.6 d is used.

If the pitch is decreased excessively, coverage may be poor due to so-called stacking. This phenomenon occurs perpendicular to the printing direction if the droplet distance goes below a critical value because the neighboring droplet on the substrate is already solidified. According to Gao and Sonin, who investigated the influence of wax droplet height and pitch on stacking, a droplet distance lower than the droplet height will lead to stacking [4]. From our experience, stacking starts at above 1300 dpi for a drop volume of ~15 pl.

		Piezo Voltage				
	$V_{droplet}$ [m/s]	85 V	90 V	95 V	100 V	105 V
F	10 µs	4,2	5,1	6,0	7,4	8,8
P	7 µs	5,1	7,0	9,0	11,8	13,8
W	4 µs	3,3	4,4	5,4	7,3	9,4

Table 1: *Droplet velocity dependent on U_{piezo} and fire pulse width. The pictures shown below correspond to the three highlighted parameter combinations.*

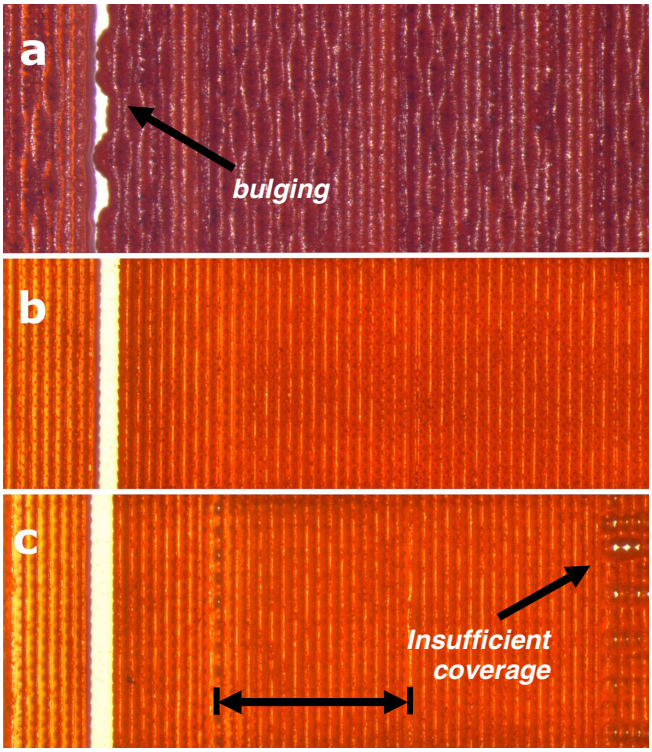

Figure 6 a: *Large droplets at a high piezovoltage led to bulging of the ink and an irregular ink surface (FPW = 10µs, 105V).* ***b:*** *Defined edges are achieved with small droplets and a moderate piezovoltage (FPW = 4 µs, 95V).* ***c:*** *Small droplets at a low piezovoltage are relatively slow with a speed of 3,3 m/s. The droplets do not form a continuous line, leaving large areas partially uncovered (FPW = 4 µs, 85V). The black bar marks the lines printed by the same Nozzle.*

Another factor for films is the shape of the piezo pulse. For each of the parameter sets in Table 1 a sample was printed on glass substrate. The temperature was left unchanged at 85°C. A mask with openings in printing direction was printed. With higher piezovoltages and thus a larger droplet the printed area becomes more irregular which results in bulging and irregular edges. We have observed that the larger the droplet is the lower is the critical voltage for this phenomenon. Low piezovoltages in combination with a short Fire Pulse Width led to insufficient line formation and thus holes in the ink layer occurred as shown in Figure 6 c. Notice, that a set of lines (app. 15 lines) printed by one nozzle may not merge whereas others do. All were triggered with exactly the same parameters, but individual nozzle characteristics result in different

behavior. Small drops with a moderate Voltage (95 V) were found to give best results. All samples were printed with the same droplet spacing.

Consequently at a given droplet size the upper limit of the resolution is stacking perpendicular to the printing direction and bulging in printing direction. The lower limit of the resolution is the need for 100% coverage.

Line openings for front contacts

For the antireflective layer on a silicon solar cell SiN is deposited using PECVD (Plasma Enhanced Chemical Vapor Deposition). SiN with refractive indexes above n = 2.1 become absorbent, whereas low refractive indexes may bring up optical losses when the solar cell is encapsulated in a solar module. To create openings in the nitride a hotmelt mask can be used as pictured in figure 1. Doing so, we found the width of openings in the nitride to exceed the printed feature considerably. Typically we find an increase of 30 to 40 microns of an opened feature for textured surfaces and a nitride refractive index around n = 2. Since the desired line width is 30 µm or below, the problem is addressed in the following.

Three mechanisms can be considered to influence undercutting:

1. Poor adhesion between SiN and the wax
2. Capillaries due to the particular surface geometry (random pyramids)
3. The wetting properties of HF-solution on SiN-layer

To investigate these effects p-doped Si-wafers featuring both a highly doped n-type emitter layer and an anisotropically etched surface with micron-scale pyramids were coated with different SiN-layers. The NH_3 / SiH_4 ratio was varied. As pictured in figure 7 an increase of the NH_3 / SiH_4 ratio leads to a decreasing refractive index of the SiN-layer (asterisk). Since we expect the wetting properties of HF-solution to be similar to water, the contact angle for water has been measured for all layers. A drop with a contact angle of 45° formed on the SiN-layer processed at a ratio of 1.5. Higher ratios led to strong wetting and insufficient drop formation with contact angles below 1° (triangle in Fig. 7).

The contact angle quantifies the ability of a liquid to wet a surface. Since strong wetting indicates good adhesion it is interesting to evaluate how the wetting behaviour of the ink itself depends on the refractive index.

So far there has not been the possibility to measure the contact angle of the molten wax. However the wetting behaviour on the different SiN layers was evaluated with liquid drops of a volume of about 1 ml (printing droplet volume: ~ 30 pl). Therefore the samples were kept at a temperature above the melting point of the wax. Just as water droplets, a liquid wax droplet formed on the SiN with a NH_3 / SiH_4 ratio of 1.5, whilst the other two samples showed large area wetting.

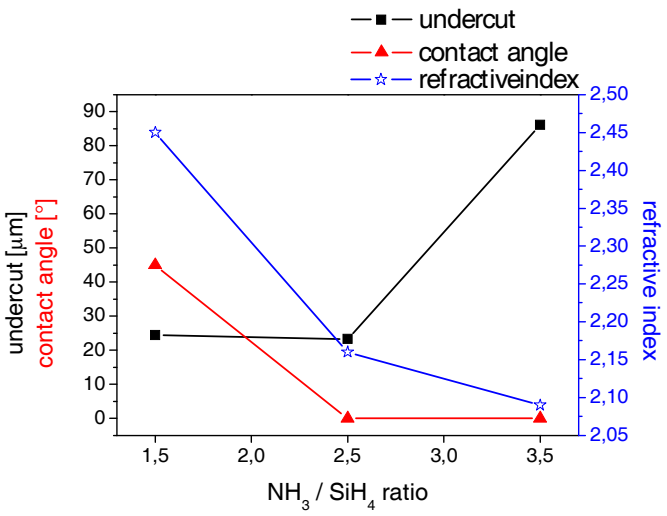

Figure 7: *Undercut, contact angle and refractive index dependent on the NH_3 / SiH_4 ratio. Refractive index and contact angle decrease for higher gas ratios. The undercut is considerably higher for a gas ratio of 3.5.*

Finally a hotmelt mask featuring line openings of ~15 µm was jetted with the same printing parameters on all wafers. The wafers were etched for 3 min in 20 % HF. The resulting line widths in the dielectric layer were measured with a microscope and the undercut was determined. The samples processed with NH_3 / SiH_4 ratios of 1.5 and 2.5 showed moderate undercutting of 25 µm, whereas strong undercutting occurred on the samples processed with a NH_3 / SiH_4 ratio of 3.5. The undercut value shown for a NH_3 / SiH_4 ratio of 1.5 represents the area where the SiN was attacked, since it could not be fully opened after 3 min.

As pictured in figure 7 the undercut does not correlate with high contact angles and hence poor adhesion. Consequently either adhesion is not responsible for undercutting or the transition from the liquid to the solid phase changes the adhesion properties of the system. For the same reason, wetting of the HF-solution does not explain the differences.

As the samples feature the same texturisation, no differences concerning the presence of capillaries can be expected. Still we observe stronger undercutting for the lowest refractive index. The reason for undercutting is subject to further investigations.

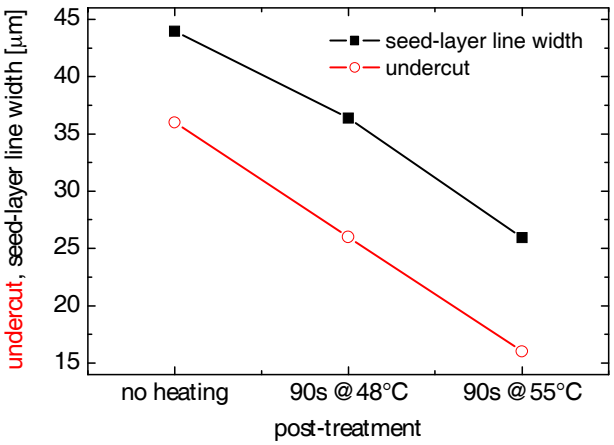

Figure 8: *Dependence of nickel seed layer width and undercut on post treatment temperature. The post treatment decreases the line width and higher temperatures lead to better results.*

The following experiments were carried out in order to obtain the narrowest front contact seed layer line width. We were able to print masks with minimal openings of ~10 µm width perpendicular to the printing direction. Due to the droplet geometry the edges were found to be wavy, and the difference between the thinnest and the thickest part of the line was 10 µm.

In order to reduce undercutting, printed wafers were heated after printing. Though the temperatures were below the melting point of ~70°C, yet a movement of the ink could be observed under a microscope. Figure 9 shows SEM images of the textured surfaces of samples processed with process b in figure 1, adding different temperature treatments after printing. The brighter areas in the image centers are caused by the Ni layer, which exclusively forms at the positions where the SiN-layer was entirely removed. The opening in the mask was 15 µm wide. Sample I was not posttreated, sample II and III were posttreated for 90 seconds at 48°C and 55°C respectively.

Figure 8 displays the line width and undercut measured within SEM-pictures, whereas 3 lines per data point were evaluated. Line widths of around 25 µm could be achieved. The post treatment decreases the line width and higher temperatures lead to better results. However, excessive temperature treatment leads to merging of the edges.

Further, in Figure 9 sample I nickel plating is visible in the valleys in-between pyramids, stretching out as wide as the Nickel plating on the unheated sample. The contact finger in Figure 9 sample III is even thinner, with Nickel in the valleys stretching out not as wide as for 48°C. Thus, the feature size increase is reduced by heating. We assume, that higher temperatures are necessary to allow the ink to flow into the bottom of the valleys in-between pyramids.

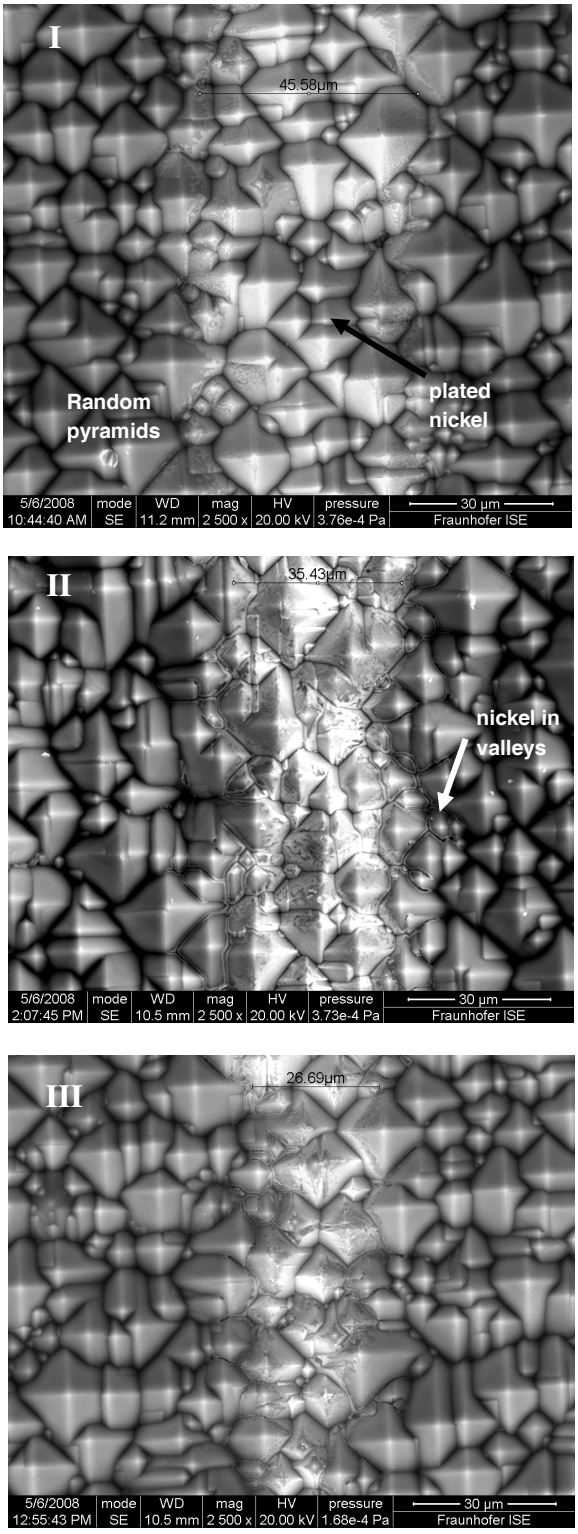

Figure 9 sample I: *The sample was not heated. Undercutting was uniform as was the subsequent nickel plating. The printed opening was 10 µm wide. Undercutting was 18 µm per edge.* ***Sample II:*** *The sample was heated to 48°C. The resulting line width was 36 µm. Undercutting was 13 µm per edge.* ***Sample III:*** *The sample was heated to 55°C. The resulting line width was 26 µm. Undercutting was 8 µm per edge.*

Conclusion

Inkjetting of a molten wax resistant to HF was evaluated for the application in next generation solar cell processing, focusing on the front contact formation.

Solidification was found to be the dominant mechanism for droplet formation on the substrate. Bulging and stacking were identified for limiting the resolution as they lead to interrupted lines or insufficient coverage respectively. Both phenomenons are dependent on drop size. Low fire pulse widths and low piezovoltages were found to create smaller drops, allowing better edge definition and smaller structures.

As for front contact formation undercutting in the range of the desired feature size was observed . The composition of the SiN layer was found to influence the undercutting. Heating the printed wax mask to temperatures below the melting point, reduces undercutting and allowed to create metal contact structures of width below 30 μm on microstructured surfaces.

References

[1] Glunz, S.W., A. Mette, M. Alemán, P.L. Richter, A. Filipovic, and G. Willeke, New concepts for the front side metallization of silicon solar cells, in Proceedings of the 21st European Photovoltaic Solar Energy Conference, Dresden, Germany, 746-9 (2006).

[2] Biro, D., D. Erath, U. Belledin, J. Specht, A. Lemke, M. Aleman, N. Mingirulli, J. Rentsch, R. Preu, R. Schlosser, B. Bitnar, and H. Neuhaus, Injet Printing for high definition industrial masking processes for solar cell production, in Technical Digest of the 17th International Photovoltaic Science and Engineering Conference, Fukuoka, Japan, (2007).

[3] Reis, N., C. Ainsley, and B. Derby, Ink-jet delivery of particle suspensions by piezoelectric droplet ejectors, Journal of Applied Physics, 97, (2005).

[4] Gao, F. and A. Sonin, Precise Deposition of Molten Microdrops: The Physics of Digital Microfabrication, Proceedings: Mathematical and Physical Sciences, 444, 533-554, (1994).

Author Biography

Dipl.-Ing. (FH) Jan Specht studied Print- and Media Technology at Stuttgart Media University. He wrote his diploma thesis on hotmelt screen printing for solar cells at Fraunhofer ISE. He has since been working with different printing technologies at Fraunhofer ISE. He now focuses on inkjet technologies